C-Curves for Lengthening of Widmanstätten and Bainitic Ferrite

JIAQING YIN, LINDSAY LEACH, MATS HILLERT, and ANNIKA BORGENSTAM

Widmanstätten ferrite and bainitic ferrite are both acicular and their lengthening rate in binary Fe-C alloys and low-alloyed steels under isothermal conditions is studied by searching the literature and through new measurements. As a function of temperature, the lengthening rate can be represented by a common curve for both kinds of acicular ferrite in contrast to the separate C-curves often presented in time-temperature-transformation (TTT) diagrams. The curves for Fe-C alloys with low carbon content show no obvious decrease in rate at low temperatures down to 623 K (350 °C). For alloys with higher carbon content, the expected decrease of rate as a function of temperature below a nose was observed. An attempt to explain the absence of a nose for low carbon contents by an increasing deviation from local equilibrium at high growth rates is presented. This explanation is based on a simple kinetic model, which predicts that the growth rates for Fe-C alloys with less than 0.3 mass pct carbon are high enough at low temperatures to make the carbon pileup, in front of the advancing tip of a ferrite plate, shrink below atomic dimensions, starting at about 600 K (323 °C).

DOI: 10.1007/s11661-017-4196-5

I. INTRODUCTION

WIDMANSTÄTTEN ferrite typically forms from austenite on cooling hypoeutectoid steels in an upper temperature range, and at lower temperature, bainite forms. Their overall rates of formation, expressed through volume fractions, are generally represented by separate C-curves in time-temperature-transformation (TTT) diagrams, although both have acicular units of ferrite as the leading phase. However, when studying the lengthening rates of units half a century ago, Hillert[1] found that they could be represented by a common model covering the entire experimental temperature range. He showed how the lengthening rates could be accounted for with a growth equation based on rate controlled by diffusion of carbon. Kaufman *et al.*[2] made a similar analysis of the same data and some additional experimental information, obtaining similar results. On the other hand, Goodenow and Hehemann[3] accepted that Widmanstätten ferrite forms under diffusion of carbon but proposed that bainitic ferrite lengthens by repeated nucleation and diffusionless growth of subunits to a limited length. They thus proposed that the lengthening rate of bainite is governed by a rate of nucleation of new subunits, which results in separate transformation curves for Widmanstätten ferrite and bainite. They did not try to account for measured lengthening rates, but the rate of nucleation and volume of subunits had later been used as fitting parameters for curves representing the rate of volume increase of bainite, *e.g.*, by Matsuda and Bhadeshia.[4] Two different hypotheses have developed from these different approaches, the diffusional and diffusionless hypotheses. They yield different predictions regarding the kinetics, and the most obvious controversy is whether there should be a common C-curve or two separate C-curves. However, the difference in opinion about the transformation mechanism mainly concerns the lengthening of the acicular units, and a kinetic test should be based on a direct study of the lengthening rate instead of the overall rate of volume increase. The volume increase is a result of many processes, *e.g.*, primary nucleation on different kinds of sites, repeated nucleation, stimulated nucleation, lengthening, widening and thickening of the acicular units, hard impingement on lengthwise growth, and soft impingement on thickening. Possibly, cementite may also have an effect, and again, this is governed by the factors mentioned previously. Finally, one should also consider the mutual stimulation of growth of one phase by the other. It is evident that information on lengthening rates would provide a more conclusive test of the proposed difference in growth mechanisms.

Today, the diffusionless mechanism seems to be most widely preferred but usually for other reasons than

JIAQING YIN, LINDSAY LEACH, MATS HILLERT, and ANNIKA BORGENSTAM are with the Department of Materials Science and Engineering, KTH Royal Institute of Technology, Stockholm 10044, Sweden. Contact e-mail: jiaqing@kth.se
Manuscript submitted December 13, 2016.
Article published online July 10, 2017

kinetic. This might primarily be because it has yielded a tool for predicting the bainite start temperature from the steel composition. The separate C-curves in TTT diagrams are still used as arguments for the diffusionless mechanism.[5] Another reason may be the widely spread conviction that the experimental growth rate is too high to be explained by the rate of carbon diffusion.[6,7] It is based on two consecutive video frames from 653 K (380 °C) by Bhadeshia,[8] who reported a growth rate of 75 μm/s as compared with a value of 0.0834 μm/s calculated for diffusion-controlled growth, *i.e.*, a deviation by three orders of magnitude. This result was again presented[6] but now illustrated with five frames and also with a graph comparing some old information with calculations for diffusional growth from Ali and Bhadeshia.[9] It showed a deviation of only about one order of magnitude for most of that information. Moreover, that was obtained with an assumed energy barrier of 400 J/mol. Without a barrier, they[9] obtained rough agreement between most of the experimental values and predictions from diffusion of carbon and that was in fair agreement with an earlier comparison by Kaufman *et al.*[2] who had examined part of the same information. The possible disagreement of kinetic information with the diffusional hypothesis will be discussed at the end of Section IV.

The primary aim of the present work was to review relevant information on lengthening rates and to make new measurements to test the validity of the old information. It is well known that the microstructure and kinetics of bainitic ferrite can be strongly affected by alloying additions. We decided to avoid unnecessary complications, and the present work was thus limited to binary Fe-C alloys and Fe-C-Mn-Si alloys with low alloy additions. The present compilation of lengthening rates of acicular ferrite may be a basis of future efforts to understand the mechanism of the lengthening process and also to rationalize lengthening information from alloyed steels.

II. EXPERIMENTAL

A. *Experimental Conditions*

Three low-alloyed steels with 0.3 mass pct carbon, hereafter denoted 0.3C, were recently used for morphological studies of Widmanstätten ferrite and bainite.[10,11] These alloys were also applied to the current study, see Table I for their chemical compositions along with the calculated T_0, T_0', and WB_s (Widmanstätten-Bainite-start) temperatures. T_0 and T_0' are calculated using Thermo-Calc[12] with the TCFE7 database and WB_s by a model developed by Kolmskog[13] coupled to Thermo-Calc. The choice of 0.3 mass pct carbon was made by balancing the wish to limit the pearlitic transformation with the wish to suppress the martensitic transformation. It was thus possible to carry out measurements over a wide range of temperatures. Isothermal treatment was applied at temperatures ranging from 1023 K to 473 K (750 °C to 200 °C) with a 50 K interval. Specimens were austenitized at 1473 K (1200 °C) for 2 hours before being manually transferred into the isothermal Bi-Sn bath, followed by final quench into iced brine. The austenitization conditions were chosen such that large grain sizes were obtained to aid subsequent measurements.

Three more alloys with different carbon contents were examined, in order to investigate the effect of the bulk carbon content on the lengthening rate. Their chemical compositions, T_0, T_0', and WB_s, are also given in Table I. Similar to the 0.3C alloys, isothermal treatment was applied to the 0.5C and 0.7C alloys, from 973 K to 573 K (700 °C to 300 °C) and 973 K to 523 K (700 °C to 250 °C), respectively. Austenitization treatment for these two binary alloys was carried out at 1373 K (1100 °C) for 10 minutes.

The thicknesses of specimens were 2 mm for the 0.3C alloys and 1.5 mm for the 0.5C and 0.7C alloys, respectively. For all the specimens, standard metallographic preparation was carried out, ending with a 0.05-μm alumina suspensions polish followed by etching with picral. The specimens were then examined with a light optical microscope (LOM). For scanning electron microscopy (SEM) study, specimens were repolished and etched with nital. The SEM study was carried out with a field emission gun–scanning electron microscope (FEG-SEM) JEOL* JSM-7800F, operated at 15 kV and with a working distance of approximately 7 mm.

*JEOL is a trademark of Japan Electron Optics Laboratory Ltd., Tokyo.

B. *Method of Measurement*

Widmanstätten and bainitic ferrite are both acicular or lathlike, and there is no accepted method to distinguish them microscopically. At all temperatures, acicular ferrite was often featherlike when nucleated on a grain boundary. Close inspection by SEM showed that, by proper sectioning, individual ferrite plates within a feather could be traced from grain boundary to growing tip without any interruption.[10] Due to the lathlike shape, it was thus possible to obtain a reasonable measure of the true length of acicular ferrite over the entire temperature range, regardless of the possible formation of cementite. Measurements were made with an interval of 50 K. For each specimen, the length of the longest plate or the largest width of a feather was measured. However, due to rapid transformation and insufficient cooling rate, the transformation may have started before isothermal conditions had been established in some specimens. The result was a coarser layer of the feather, in a region close to the grain boundary. An example is shown in Figure 1. This effect is most pronounced for low holding temperatures. Instead, in specimens from high temperatures, a ferrite plate may continue to grow during the final quench and sometimes form an extremely thin tip. Efforts were made to exclude such parts when measuring the length.

Primarily, the lengths of ferrite plates (laths) were measured in order to obtain information on the lengthening rate for the specific purpose of studying the

Table I. Chemical Composition (Mass Pct) of Fe Alloys and Calculated T_0 and T_0' by Thermo-Calc;[12] the WB_S Is Calculated with a Model Developed by Kolmskog[13] Coupled to Thermo-Calc

Alloy	C	Si	Mn	T_0	T_0'	WB_S
0.3CSi	0.28	0.52	0.06	976 K (703 °C)	883 K (610 °C)	1050 K (777 °C)
0.3CMn	0.27	0.03	0.45	963 K (690 °C)	872 K (599 °C)	1018 K (745 °C)
0.3CMnSi	0.26	0.51	0.48	972 K (699 °C)	878 K (605 °C)	1034 K (761 °C)
0.18CMnSi	0.18	0.31	0.47	1010 K (737 °C)	905 K (632 °C)	1055 K (782 °C)
0.5C	0.50	0.031	0.003	886 K (613 °C)	810 K (537 °C)	984 K (711 °C)
0.7C	0.70	0.033	0.003	818 K (545 °C)	748 K (475 °C)	939 K (666 °C)

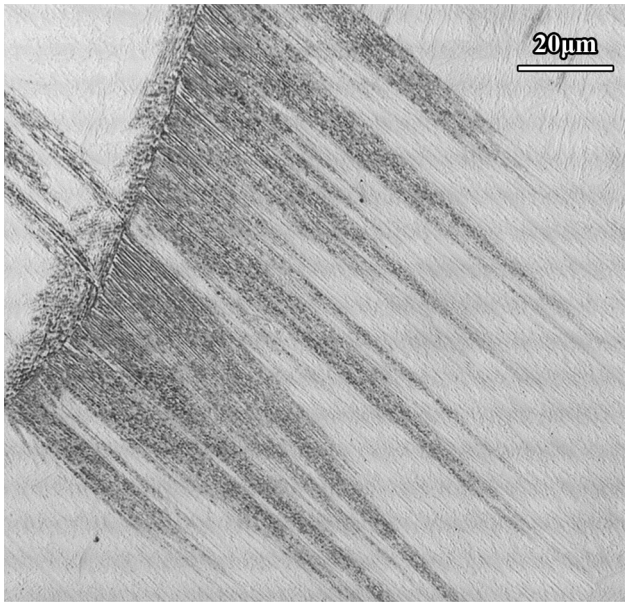

Fig. 1—Light optical micrograph showing upper bainite with coarser structure close to the grain boundary formed before the holding temperature was reached; 0.3CSi alloy held at 673 K (400 °C) for 2 s.

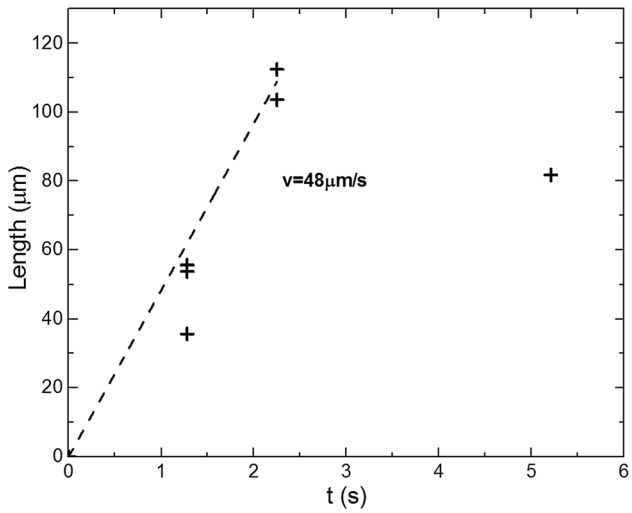

Fig. 2—Linear fitting for evaluation of the lengthening rate; alloy 0.3CSi treated at 623 K (350 °C).

variation with temperature. It was not essential to ascertain a high accuracy as long as the same method was used for different alloys and, in particular, for different temperatures. There is a natural variation of plate lengths within a specimen and within a polished section, which occurs due to several factors, including the difference of incubation time, soft and hard impingement, and finally different angles of sectioning with reference to the main growth direction of the plate. These factors were neglected by simply recording the longest plate that could be observed within a large inspected area. Such objects were located with an LOM by exploring the prepared surface and, for alloy 0.3CSi measurements, were first taken with an LOM and again after switching to SEM. There was sufficient agreement and the other alloys were measured only in an LOM. The measurements were taken from the grain boundary to the tip. It was not possible to measure the lengths of individual subunits of the kind originally proposed by Goodenow and Hehemann.[3] As shown in a detailed characterization of the ferrite plates in a parallel SEM study,[10] the primary plates of ferrite grew without any sign of interruption from the nucleation site at a grain boundary to the advancing tip in the austenite. The time of transformation was recorded with a stopwatch by starting the count when the specimen hits the Bi-Sn bath and stopping it when the specimen hits the iced brine. The accuracy was not high and was estimated to be of the order of 0.5 seconds. Incubation times of that order were thus neglected by using the origin.

As an example, Figure 2 from alloy 0.3CSi at 623 K (350 °C) was evaluated from the straight line drawn from the origin to the points at about 2 seconds. The line was well supported by the points at about 1 second, which yields some support for the neglect of the incubation time by fitting to the origin. The point at about 5 seconds was neglected because it was expected to be subject to impingement. In Figure 3, for the same alloy at 1023 K (750 °C), the straight line through the origin was supported by points at about 30 and 100 μm, and again, information from much longer time was neglected. For the 0.5C and 0.7C, the driving force and growth rate are relatively smaller than for the 0.3C. The measurements thus covered longer times and the incubation time could be much longer than the estimated uncertainty of 0.5 seconds and could no longer be neglected. The lengthening rate was then evaluated by linear fitting to the experimental points, as illustrated in Figure 4. Furthermore, due to the strong interference of pearlite formation in these two alloys, it was not possible to measure the lengthening rate of acicular ferrite at 873 K (600 °C) and 923 K (650 °C).

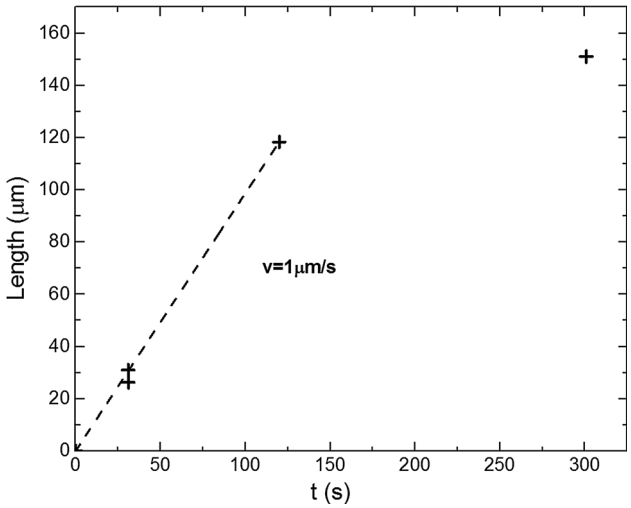

Fig. 3—Linear fitting for evaluation of the lengthening rate; alloy 0.3CSi treated at 1023 K (750 °C).

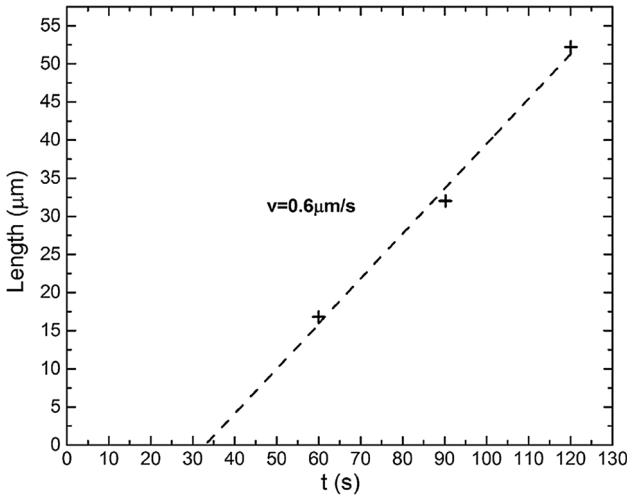

Fig. 4—Evaluation of incubation time and lengthening rate; alloy 0.7C treated at 973 K (700 °C).

III. RESULTS

The measured lengthening rates are presented in Figure 5. They do not at any temperature show a sharp change that could indicate a transition of transformation mode upon decreasing temperature for any of the alloys. The differences between the three 0.3C alloys with different alloy contents indicate that 0.5 mass pct Mn delays the lengthening rate by a factor of 1.5 to 2, and the effect of 0.5 mass pct Si seems to be negligible. An interesting feature is that for the three 0.3C alloys, there is only a weak or no indication of a maximum in the lengthening rate and the expected decrease of the lengthening rate at lower temperatures is hardly noticeable within the experimental range of temperature. This result seemed hard to explain with a diffusion-controlled transformation. One would normally expect a C-curve behavior with a pronounced decrease of rates below a nose due to decreasing diffusivity.

Initially, it was suspected that a considerable part of a plate in a specimen transformed at a low holding temperature could have formed during cooling through a higher temperature range with higher growth rates, which would result in a longer plate than normal for the holding temperature. The effect should be smaller in thinner specimens that cool quicker. Micrographs in a classic article by Modin[14] were thus examined, because his 0.8-mm specimens were thin in comparison to the 2-mm specimens used in the present experiments. Information obtained from his micrographs was encouraging but too meagre. Luckily, his old specimens could be located and were reexamined. The alloy had 0.18 mass pct C and is listed as the 0.18CMnSi in Table I. Unfortunately, his specimens from 873 K (600 °C) were missing. The results of measurements are presented in Figure 5 and show a very similar behavior. Considering that these specimens were only 0.8 mm, it seems that the larger thickness of specimens of the other alloys was not the cause of the unusual behavior. In order to verify this behavior, some old values from Hillert[1] are presented in Figure 6, together with the new results with carbon contents lower than 0.45 mass pct C, and they show the same behavior. Simonen *et al.*[15] made a careful study of lengthening rates in binary Fe-C alloys, and their results are also included in Figure 6 and are in general agreement. They still show no decrease of rates at their lowest temperature, 723 K (450 °C). Results for higher carbon contents are collected in Figure 7. Data for 0.81 mass pct carbon from Hillert together with 0.91 mass pct carbon from Hawkins and Barford[16] show the normal decrease of rates below a nose temperature of about 800 K (523 °C), and data for 0.5 and 0.7 mass pct carbon from the present study show that the tendency for decreasing rates at low temperatures is evident already at these carbon contents. The abnormal behavior seems to be limited to low carbon contents.

In principle, more reliable information could be obtained by direct observations of growth in a microscope with hot stage, but such information has been limited to high carbon contents due to the rapidity of the transformations involved. Moreover, such studies have been limited to low temperatures. In recent years, it has become possible to carry out hot-stage measurements at much higher temperatures, and one is able to capture the rapid growth with a high-speed camera.[17,18] Unfortunately, most of those works so far have focused on the lengthening rate either at a lower temperature range or with much higher alloy steels than is of interest in the current study. Using an Fe-C alloy with 0.91 mass pct C, Hawkins and Barford[16] examined the lengthening rate up to 673 K (400 °C). Their results are also presented in Figure 7 and show the expected decreasing lengthening rates at lowering temperatures.

Yada and Ooka[19] also observed a wide C-curve for the lengthening rate of acicular ferrite in a Fe-6Ni-0.29C (in mass pct) alloy by hot-stage microscopy. In contrast, a pronounced decrease of the lengthening rate below a nose was observed in three other alloys with more than 0.48 mass pct C (Figure 4 in Reference 19).

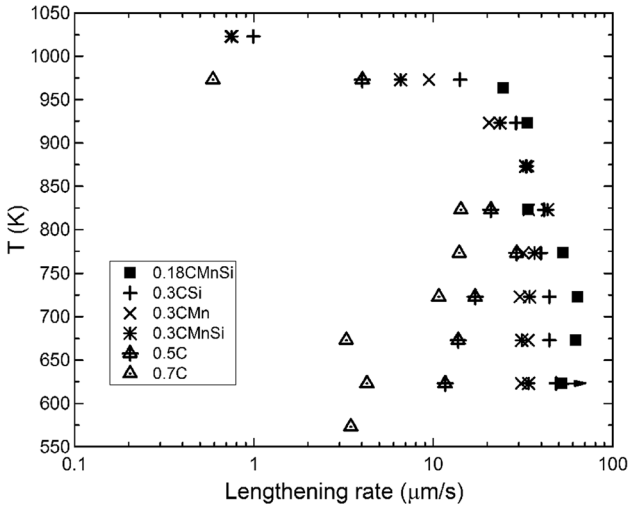

Fig. 5—Measured lengthening rate of acicular ferrite in the current study. The arrow indicates that the point has possibly been underestimated since intragranular ferrite plate formed intensively at this temperature in alloy 0.18CMnSi, which gives hard impingement to ferrite plates.

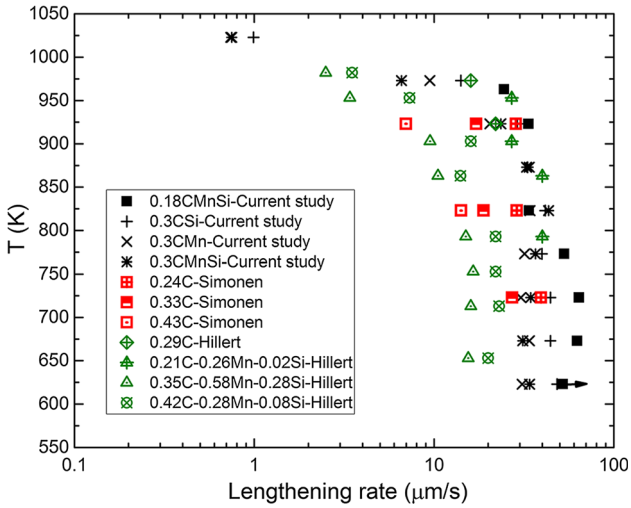

Fig. 6—Comparison of lengthening rate data obtained in the current study with those reported by Hillert[1] and Simonen *et al.*[15] in alloys with carbon contents lower than 0.45 mass pct.

IV. MODELING LENGTHENING RATE UNDER FULL LOCAL EQUILIBRIUM

So far, it has been shown that the new experimental data are consistent with other experimental reports. It remains to be tested how the data compare with predictions from available models. However, according to the diffusionless model, the growth rate depends on the rate of nucleation of subunits, which is hypothetical and is used as a fitting parameter (*e.g.*, Matsuda and Bhadeshia[4] and Liu *et al.*[20]) Hence, the test can only be made with the diffusional model. It also has an unknown factor because it is now well established that bainitic ferrite can be considerably supersaturated with carbon. That will now be neglected but will be further discussed in Section VI.

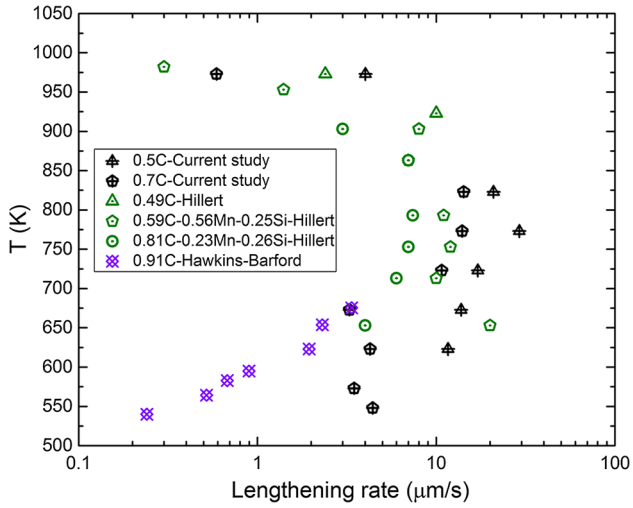

Fig. 7—Comparison of lengthening rates at higher carbon contents obtained in the current study with those reported by Hillert[1] and Hawkins and Barford[16] in alloys with carbon contents of approximately 0.5 mass pct or higher.

The lengthening equation under diffusion control is described according to the approach by Zener and Hillert, which is often called the Zener–Hillert model. The original model[21] has recently been modified.[22] A previous approximation of the driving force as $RT(x_{eq}^{\gamma/\alpha} - x^{\gamma_o})$ was removed. Zener[23] proposed that the maximum growth rate occurs at an optimal radius equivalent to $2\rho_{cr}$, where ρ_{cr} is the critical radius of curvature. The criterion that the sharpness of the plate tip adjusts to an optimal value at which the rate is maximum is still maintained, but the coefficient to ρ_{cr} will no longer have a constant value. For a more concise explanation of the alterations, the reader is referred to the publication by Leach *et al.*[22] The modified equation is

$$v = \frac{D\Delta G_m^o / V_m}{2\sigma} \frac{x^{\gamma/\alpha} - x^{\gamma_o}}{x^{\gamma_o} - x^{\alpha/\gamma}} \frac{\rho_{cr}}{\rho} \qquad [1]$$

where v is the lengthening rate; D is the diffusion coefficient of carbon in austenite; V_m is the molar volume of ferrite; σ is the specific interfacial energy; $x^{\gamma/\alpha}$ and $x^{\alpha/\gamma}$ are the mole fractions of carbon in austenite and ferrite, respectively, at the austenite/ferrite interface; x^{γ_o} is the alloy carbon content; and ρ is the actual radius of curvature. Equation [1] is an expression for the rate at any radius of curvature, and the point of interest is the maximum growth rate attained at the optimal radius, which is obtained by an iterative process starting from the critical radius, ρ_{cr}.

Equation [1] was now applied for predicting the lengthening rates of acicular ferrite in Fe-C alloys of various carbon contents (Figure 8). Extrapolation of the A_3 line was obtained through thermodynamic calculations using thermodynamic information from the TCFE7 database in the Thermo-Calc software,[12] and diffusion data for carbon in austenite were taken from Ågren's[24] extrapolation of experimental data by Wells *et al.*[25] All that information is obtained by long

extrapolations in temperature and carbon content. For the ferrite/austenite interface, a value 0.2 J/m^2 was used, which is also uncertain. One should thus not expect predicted growth rates from Eq. [1] to be extremely accurate. Since diffusivity is a function of the carbon content, three kinds of diffusivities were considered: one type, D_0, was calculated for the alloy carbon content x^{γ_o}; another one was the maximum diffusivity, $D_{\max}$, calculated for the carbon content at the interface $x^{\gamma/\alpha}$; and, finally, the effective diffusivity, D_{eff}, was, according to Trivedi and Pound,[26]

$$D^{\text{eff}} = \frac{1}{x^{\gamma/\alpha} - x^{\gamma_0}} \int_{x^{\gamma_0}}^{x^{\gamma/\alpha}} D(x) \qquad [2]$$

In addition to the preceding uncertainties, the method of calculating the effective diffusion coefficient will be different for different geometries, and Trivedi and Pound considered diffusion in one dimension, whereas for edgewise growth of a plate, it is two dimensional. This difference will be more important at a stronger dependence of composition. The calculated widths of the curves in Figure 8 vary considerably with the choice of diffusivity. Already in the recent work of Leach *et al.*,[22] it was shown that the strong composition dependence of the diffusivity of carbon in austenite results in a widening of the predicted C-curve, which they noted with satisfaction because they were already aware of the experimental C-curves being extremely wide. The reason is that the carbon content in local equilibrium with ferrite will increase with lowering temperature and may partly balance the natural decrease of the diffusivity with decreasing temperature. It was now realized that this effect on the C-curve would be more pronounced if it is assumed that the effective diffusivity falls even closer to the maximum value in the diffusion field, *i.e.*, for the local equilibrium composition.

The curve for 0.9 mass pct carbon in Figure 8, obtained with the effective diffusivity, the solid line, reproduces the experimental values for 0.81 and 0.91 mass pct carbon in Figure 7 fairly well, especially the slope at low temperatures (Figure 9). In spite of all the preceding uncertainties, this lends some support to the diffusional model and, in particular, to the use of the effective diffusivity defined by Trivedi and Pound.[26] The large discrepancy, mentioned in Section I, may mainly depend on the long extrapolations of diffusivity and thermodynamic information. Hu *et al.*[27] recently examined a steel, similar to the one studied by Bhadeshia,[6] Fe-0.4C-2Si-2.81Mn compared to Fe-0.42C-2.02Si-3Mn. They measured only 8 μm/s during cooling from 683 K to 671 K (410 °C to 398 °C), which was close to the same temperature, 653 K (380 °C). This rate is lower than all the data in the same temperature range for binary Fe-C alloys and alloys with low alloy contents in Figure 6, which might be due to the alloying elements. It seems that the diffusional mechanism could not be discarded on kinetic grounds.

On the other hand, the special character of the curves for low carbon contents is not reproduced, which is illustrated by the comparison with experimental information for 0.3 mass pct carbon in Figure 10. Even though the width of the curves varies with the choice of diffusivity, the small or absent decrease of a rate at lower temperatures within the experimental temperature range is not reproduced by any curve, and that result is independent of the preceding uncertainties. One may feel that the agreement would be least unsatisfactory for the maximum diffusivity. The use of maximum diffusivity was recommended by Wagner[28] and accepted by Hillert[29] with the additional argument that for the lengthening of ferrite plates, the maximum value occurs

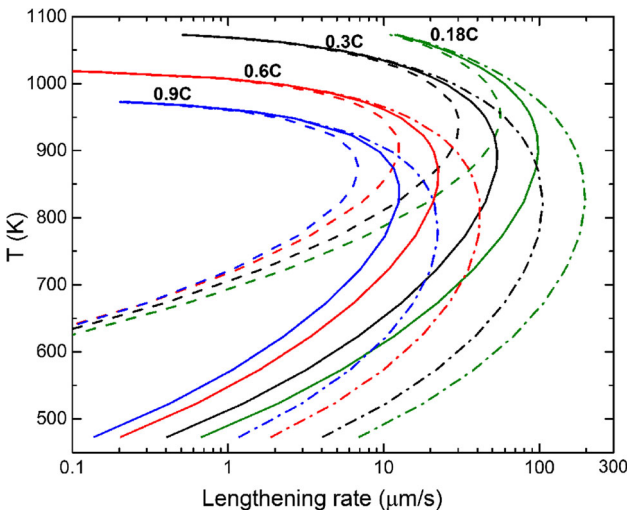

Fig. 8—The lengthening rate of acicular ferrite with various carbon contents predicted by the modified Zener–Hillert model. The dashed, solid, and dash-dotted lines represent the growth rates calculated by applying the diffusivities D_0, D_{eff}, and $D_{\max}$, respectively.

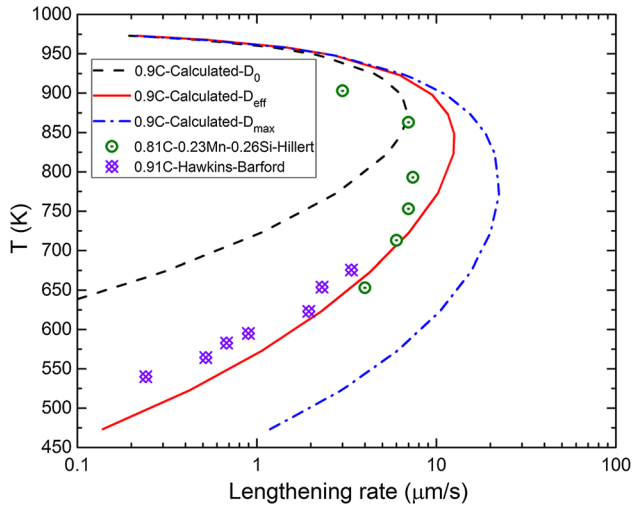

Fig. 9—Comparison of experimental lengthening rates for the 0.81C[1] and 0.91C[16] alloys and the calculated ones with the modified Zener–Hillert model for Fe-0.9C alloy.

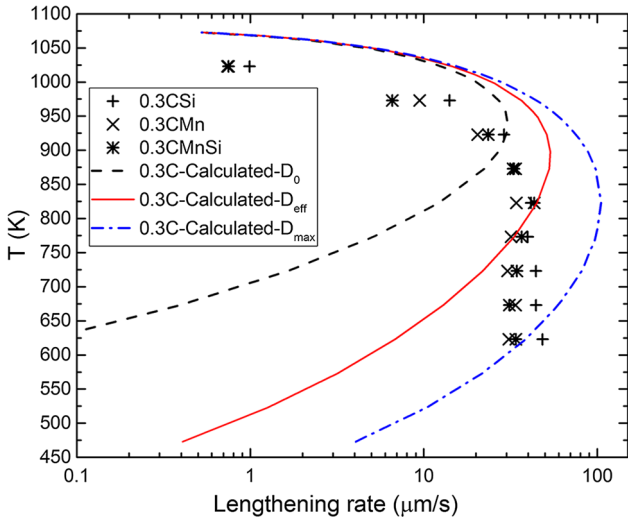

Fig. 10—Comparison of experimental lengthening rates for the three 0.3C alloys and calculated ones with the modified Zener–Hillert model for Fe-0.3C alloy.

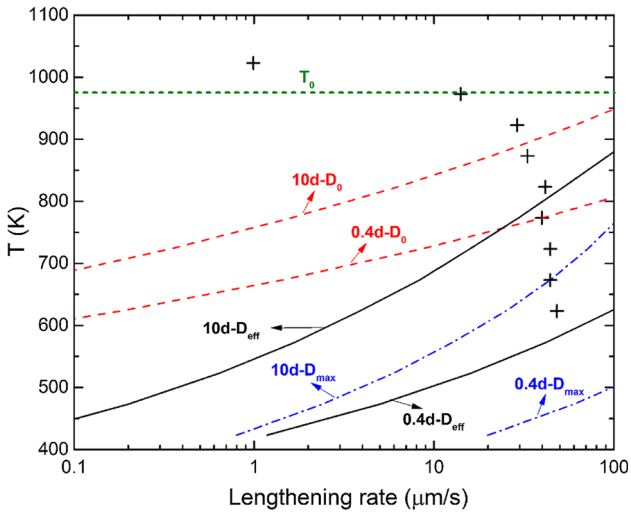

Fig. 11—Prediction of critical rate for transition from diffusional to diffusionless with varying temperature. Three choices of carbon diffusivity were considered. For each choice of carbon diffusivity, deviation from chemical equilibrium is expected when the growth rate exceeds the 10 d line. Similarly, transition from diffusional to diffusionless is expected when the rate exceeds the 0.4 d line. The experimentally determined growth rate and the T_0 are given for the 0.3CSi alloy.

in contact with the tip where the cross section for the diffusional flow is smallest. As already mentioned, the effective diffusivity was derived by Trivedi and Pound[26] for a one-dimensional diffusion field, which is much different from the diffusion field around the top of a plate. However, for better agreement, it would be necessary to make the calculated nose much flatter but maybe not wider. It is evident that the nearly constant lengthening rate at lower temperatures cannot be explained with rate control, only by diffusion of carbon.

V. MODEL OF DEVIATION FROM LOCAL EQUILIBRIUM

When searching for the effect making the calculated nose much flatter, we decided to explore the possibility that there is an increased deviation from local equilibrium at the tip of acicular ferrite at decreasing temperature. Zener[23] already discussed the possibility of an increasing deviation from local equilibrium at the ferrite/austenite interface as the temperature was lowered. He suggested that lower bainite would finally form as a diffusionless product at low temperatures. With his model, Hillert[1] demonstrated that at constant temperature, there can be a critical carbon content of the alloy below which the growth of ferrite turns diffusionless. Ågren[30] developed this model further.

When discussing the growth of ferrite in FeCX alloys, Hillert[31] applied a simple model for the transition to partitionless growth, which was supposed to produce so-called paraferrite[32] with the same alloy content as the parent austenite. He estimated the width of a pileup of ejected alloying element in front of an advancing phase interface as D/v and proposed that a noticeable deviation from local equilibrium would begin when it turns into a thin spike for $D/v < 10\ d$, while close to ideal paraequilibrium would be obtained for $D/v < 0.4\ d$, where d was the distance between atomic planes. Coates[33] later proposed the limits $D/v < 2.5$ nm and $D/v < 0.5$ nm. The same simple model will now be applied to interstitial carbon in austenite where the distance between interstitial sites is $d = 0.25$ nm. As for the prediction of lengthening rates, it is again not evident what diffusivity for carbon in austenite should be used. This may be a particularly intricate problem when the diffusion field is not one dimensional. The same three alternatives as in Figures 8, 9, and 10 were applied to the growth of ferrite in an alloy with 0.3 mass pct C. The results are presented in Figure 11 together with the experimental results for the 0.3CSi alloy.

In Figure 11, there are two solid curves for the effective diffusivity, and the lower one is formally the critical line below which one could expect strong deviation from local equilibrium at the advancing ferrite/austenite interface. For the 0.3CSi alloy, it would occur just below the last experimental point. The upper solid curve indicates that deviation from local equilibrium could start already at 800 K (527 °C) in this alloy. Note that the width of the carbon spike in front of an advancing tip of ferrite was here based on one-dimensional diffusion and a constant diffusion coefficient. Numerical simulation of more realistic situations would be most welcome.

Since the present model is crude and the numerical values of various parameters are uncertain, the result may be taken only as an indication that the shapes of C-curves for low carbon steels may be affected by an increasing deviation from local equilibrium, as suggested by Zener.[23] This possibility has been discussed, *e.g.*, by Yada and Ooka[19] who observed a similar effect in a high Ni steel with low carbon content. If there is such a deviation from local equilibrium, it should certainly result in an increasing supersaturation of the

growing ferrite, although this simple model cannot make that kind of prediction. Such an effect would decrease the requirement for rejection of carbon and thus result in less carbon diffusion during growth. That would yield higher growth rates than predicted by Eq. [1] for full local equilibrium and could explain the unusual shapes of the C-curves for low-carbon steels. However, the decisive factor would probably not be the low carbon content but the high growth rate. The deviation from local equilibrium would be less likely for steels with higher carbon content due to their lower growth rates, which is well demonstrated by Figure 7. Additions of alloying elements may decrease the growth rates even more. From this point of view, it seems impossible that deviation from local equilibrium for carbon at the growing tip of acicular ferrite could have a decisive effect on the growth of bainite in general.

Accepting the results of the model, obtained with the effective diffusivity, as defined by Trivedi and Pound, it seems that the model will formally predict that diffusionless growth may occur beneath the last experimental point for the alloy with 0.3 mass pct carbon. On the other hand, this is difficult to test due to martensite formation. As already mentioned, the problem connected to a solute spike has occurred for the transition to growth under paraequilibrium in Fe-C-X alloys, and it can be solved only with a more sophisticated model.[34] However, there may be an important difference because the atomic structure of the moving interface would probably have a negligible effect on the carbon spike, because carbon atoms are mobile compared to the substitutional solutes in the bcc lattice and probably also in the disturbed lattice of an interface. It may not matter much if the phase change occurs by a displacive mechanism or by a partly reconstructive mechanism such as the one presented by Aaronson *et al.*[35]

VI. COMPARISON WITH DIFFUSIONLESS MODEL

There have been many studies of the supersaturation of carbon in bainitic ferrite, initially performed by X-ray diffraction and later dominated by the atomic probe technique. This is an essential feature of the diffusionless model, which predicts that ferrite should inherit all the carbon of the parent austenite. Supersaturation has been repeatedly confirmed over the years, *e.g.,* References 36 through 38. The experimental technique has gradually improved, and several such papers of admirable quality have appeared recently.[39,40] Today, it seems to be a well-established fact that some carbon in bainitic ferrite is dissolved in the defect-free parts, but most is present as clusters or at dislocations. For the diffusionless model, it is of interest whether all the carbon content has been trapped; however, that is difficult to test because supersaturated carbon in ferrite may immediately start to partition into austenite. For the diffusional model, it is an interesting question what fraction of the carbon content of the parent austenite is not dissolved in the ferrite, because only that amount of carbon must diffuse away from the advancing ferrite/austenite interface and will thus limit the growth rate. The growth rate predicted from the diffusional rate equation will be higher the smaller that fraction is. To a first approximation, it is inversely proportional to that fraction of carbon. In the present work, the growth rates were predicted under the assumption that all the carbon in the parent austenite must diffuse away. To increase the growth rate markedly, it is necessary that the fraction retained in the ferrite plate is large, *i.e.*, that the growth is virtually diffusionless.

Information on the low content of carbon in the defect-free ferrite is also of interest for the diffusional model but only if it is established already by the growth mechanism and is not the result of a later redistribution because the chemical potential of all the carbon trapped in the growing ferrite is controlled by that content. Even without a detailed model, it may be concluded that with a lower carbon content in the defect-free part of ferrite, a lower deviation from local equilibrium at the advancing interface has been required. It is an interesting question whether a future unified model will have more characteristics of the diffusionless or diffusional model.

VII. CONCLUSIONS

1. For hypoeutectoid Fe-C alloys, it has been confirmed that the lengthening rates of Widmanstätten ferrite or bainitic ferrite as functions of temperature can be represented by a common C-curve.
2. It is suggested that the separation of kinetic information on acicular ferrite into two curves, which has often been reported for TTT diagrams, should not be accepted as an indication of different growth mechanisms but of complex kinetic factors governing the volume fractions.
3. Using the effective diffusivity for carbon, as defined by Trivedi and Pound,[26] predictions from the growth rate equation for diffusional growth in an Fe-0.9C alloy are supported by measurements on alloys with 0.81 and 0.91 mass pct carbon down to 573 K (300 °C).
4. Virtually, the temperature-independent lengthening rate of bainite at low temperatures was observed in an old study of low-alloyed, hypoeutectoid steels.[1] It has now been confirmed by a new series of measurements, but it occurs only in low carbon steels.
5. A simple model of the carbon spike in front of the advancing tip of acicular ferrite has been applied. It indicates when a deviation from local equilibrium can be expected, which is the case at the lowest experimental temperature for Fe-0.3C alloys. It is proposed that this is the explanation as to why the growth rate has not decreased there. In that case, the effect would be coupled to the high growth rate relative to the diffusivity of carbon and can only indirectly be an effect of the low carbon content.
6. This simple model describes a rate-dependent deviation from local equilibrium under the conditions where this effect has been observed, but it does not describe the possible supersaturation due to the deviation.

ACKNOWLEDGMENTS

The authors acknowledge the financial support from VINNOVA, the Swedish Governmental Agency for Innovation Systems, Swedish Industry, and the KTH Royal Institute of Technology. The work has been performed within the VINN Excellence Centre Hero-m. Two Fe-C alloys investigated in this work were kindly offered by Dr. I. Zuazo, Arcelor Mittal Maizieres Research (S.A.). One of the authors (JY) also thanks the China Scholarship Council (CSC) for sponsorship of this study.

REFERENCES

1. M. Hillert: "The Growth of Ferrite, Bainite and Martensite," Internal Report, Swedish Institute for Metal Research, Stockholm, 1960, appeared in *Thermodynamics and Phase Transformations, The Selected Works of Mats Hillert,* J. Ågren, Y. Bréchet, C. Hutchinson, J. Philibert, and G. Purdy, eds., EPD Science, Les Ulis, Cedex, France, 2006, pp. 111–58.
2. L. Kaufman, S.V. Radcliffe, and M. Cohen: in *Decomposition of Austenite by Diffusional Processes*, V.F. Zackay and H.I Aaronson, eds., Interscience, New York, 1962, pp. 313–52.
3. R.H. Goodenow and R.F. Hehemann: *Trans. AIME*, 1965, vol. 233, pp. 1777–86.
4. H. Matsuda and H.K.D.H. Bhadeshia: *Proc. R. Soc. London A*, 2004, vol. 460, pp. 1707–22.
5. Y. Ohmori, H. Ohtsubo, K. Georgima, and N. Maruyama: *Mater. Trans. JIM*, 1993, vol. 34, pp. 216–23.
6. H.K.D.H. Bhadeshia: *Bainite in Steels*, 3rd ed., Maney Publishing, Wakefield, United Kingdom, 2015.
7. L.C.D. Fielding: *Mater. Sci. Technol.*, 2013, vol. 29, pp. 383–99.
8. H.K.D.H. Bhadeshia: in *Phase Transformations in Ferrous Alloys,* A.R. Marder and J.I. Goldstein, eds., ASM, Cleveland, OH, 1984, pp. 335–40.
9. A. Ali and H.K.D.H. Bhadeshia: *Mater. Sci. Technol.*, 1989, vol. 5, pp. 398–402.
10. J. Yin, M. Hillert, and A. Borgenstam: *Metall. Mater. Trans. A*, 2017, vol. 48A, pp. 1425–43.
11. J. Yin, M. Hillert, and A. Borgenstam: *Metall. Mater. Trans. A*, 2017, vol. 48A, pp. 1444–58.
12. J.O. Andersson, T. Helander, L. Höglund, P.F. Shi, and B. Sundman: *Calphad*, 2002, vol. 26, pp. 273–312.
13. P. Kolmskog: Ph.D. Thesis, KTH, Stockholm, 2013.
14. S. Modin: *Jernkont. Ann.*, 1958, vol. 142, pp. 37–80.
15. E.P. Simonen, H.I. Aaronson, and R. Trivedi: *Metall. Trans.*, 1973, vol. 4, pp. 1239–45.
16. M.J. Hawkins and J. Barford: *J. Iron Steel Inst.*, 1972, vol. 210, pp. 97–105.
17. X.L. Wan, R. Wei, L. Cheng, M. Enomoto, and Y. Adachi: *J. Mater. Sci.*, 2013, vol. 48, pp. 4345–55.
18. L. Cheng, K.M. Wu, X.L. Wan, and R. Wei: *Mater. Charact.*, 2014, vol. 87, pp. 86–94.
19. H. Yada and T. Ooka: *J. Metall. Soc. Jpn.*, 1967, vol. 31, pp. 766–71.
20. C. Liu, L. Shi, Y. Liu, C. Li, H. Li, and Q. Guo: *J. Mater. Sci.*, 2016, vol. 51, pp. 3555–63.
21. M. Hillert: *Jernkont. Ann.*, 1957, vol. 147, pp. 757–89.
22. L. Leach, M. Hillert, and A. Borgenstam: *Metall. Mater. Trans. A*, 2015, vol. 46A, pp. 19–25.
23. C. Zener: *Trans. AIME*, 1946, vol. 167, pp. 550–83.
24. J. Ågren: *Scripta Metall.*, 1986, vol. 20, pp. 1507–10.
25. C. Wells, W. Batz, and R.F. Mehl: *Trans. AIME*, 1950, vol. 188, pp. 553–60.
26. R. Trivedi and G.M. Pound: *J. Appl. Phys.*, 1967, vol. 38, pp. 3569–76.
27. Z. Hu, G. Xu, H. Hu, L. Wang, and Z. Xue: *Int. J. Miner. Metall. Mater.*, 2014, vol. 21, pp. 371–78.
28. C. Wagner: *Trans. TMS-AIME*, 1952, vol. 194, p. 91.
29. M. Hillert: *Acta Metall.*, 1959, vol. 7, pp. 653–58.
30. J. Ågren: *Acta Metall.*, 1989, vol. 37, pp. 181–89.
31. M. Hillert: "Paraequilibrium," Internal Report, Swedish Institute for Metal Research, Stockholm, 1953, appeared in *Thermodynamics and Phase Transformations, The Selected Works of Mats Hillert,* J. Ågren, Y. Bréchet, C. Hutchinson, J. Philibert, and G. Purdy, eds., EPD Science, Les Ulis, Cedex, France, 2006, pp. 9–24.
32. A. Hultgren: *Jernkont. Ann.*, 1951, vol. 135, pp. 403–94.
33. D.E. Coates: *Metall. Trans.*, 1972, vol. 3, pp. 1203–12.
34. J. Odqvist, M. Hillert, and J. Ågren: *Acta Mater.*, 2002, vol. 50, pp. 3213–27.
35. H.I. Aaronson, T. Furuhara, M.G. Hall, J.P. Hirth, J.F. Nie, G.R. Purdy, and W.T. Reynolds, Jr: *Acta Mater.*, 2006, vol. 54, pp. 1227–32.
36. H.K.D.H. Bhadeshia and A.R. Waugh: *Acta Metall.*, 1982, vol. 3, pp. 775–84.
37. F.G. Caballero, M.K. Miller, S.S. Babu, and C. Garcia-Mateo: *Acta Mater.*, 2007, vol. 55, pp. 381–90.
38. F.G. Caballero, M.K. Miller, and C. Garcia-Mateo: *Acta Mater.*, 2010, vol. 58, pp. 2338–43.
39. E.V. Pereloma: *Mater. Sci. Technol.*, 2016, vol. 32, pp. 99–103.
40. R. Rementeria, J.D. Poplawsky, M.M. Aranda, W. Guo, J.A. Jimenez, C. Garcia-Mateo, and F.G. Caballero: *Acta Mater.*, 2017, vol. 125, pp. 359–68.